5-1-2010

The Development of a Comprehensive Mechanism for Intracellular Calcium Oscillations: A Theoretical Approach and an Experimental Validation

Amanda A. Borges
Salve Regina University, amanda.borges@salve.edu

Deanna Salter
Salve Regina University, deanna.salter@salve.edu

Sandor Kadar
Salve Regina University, kadars@salve.edu

Steven B. Symington
Salve Regina University, steven.symington@salve.edu

2010

The Development of a Comprehensive Mechanism for Intracellular Calcium Oscillations: A Theoretical Approach and an Experimental Validation

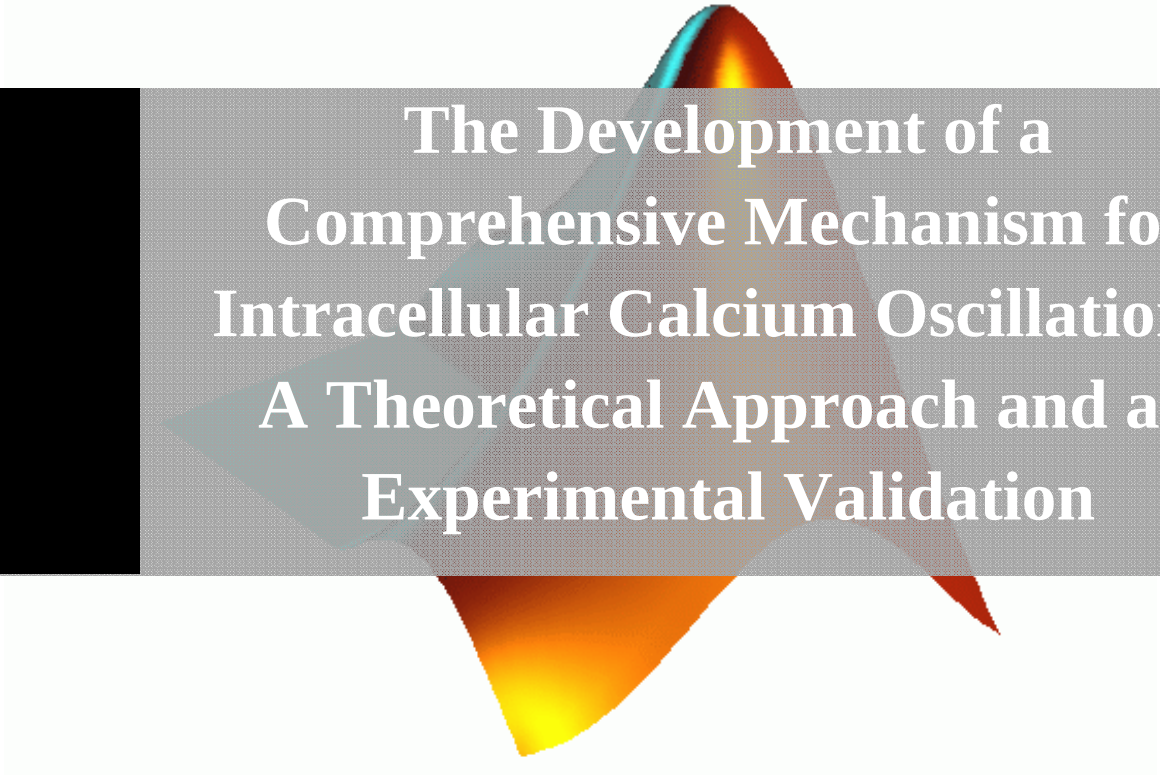

Amanda Borges[1] , Deanna Salter[2], Sándor Kádár[1], Steven B. Symington[2]
[1]Department of Chemistry,
[2]Department of Biology and Biomedical Sciences
Salve Regina University, Newport, RI 02840

This Research was made possible by RI-INBRE Grant # P20RR016457 from the National Center for Research Resources (NCRR), a component of the National Institutes of Health (NIH).” and “Its contents are solely the responsibility of the authors and do not necessarily represent the official views of NCRR or NIH.

I would also like to thank my mentor Dr. Sándor Kádár for getting me involved in this research project, supporting me throughout this entire process, and broadening my horizons.

Additional thanks to Dr. Steven B. Symington, and Deanna Salter ’10 for their contribution of experimental data, in addition to their time, patience, and assistance.

Table of Contents

I- Basis for Development of the Model

A. Importance of Mathematical Modeling:

A thorough understanding of the interaction between molecules, processes, and pathways is necessary to understand complex biological systems such as cells and tissues. In the past, research of biological systems focused on empirical approaches, which used numerical models that described the behavior of the processes in a vacuum. Due to this approach, there was a disconnection between biologists, chemists, and mathematicians. Biologists now turn to chemical systems for numerical models because biological systems are exceptionally complex and chemical systems are simpler, manageable, and readily available. Advancements in biological and computational techniques enable researchers to monitor complex cellular processes on the molecular level. Computational models are important because they allow researchers to investigate how individual complex regulatory processes operate. In addition, they are beneficial in the analysis of how the processes are interconnected and how disruptions of these processes may contribute to the development of a disease. Computational models are also beneficial for developing hypotheses to guide the design of new experimental tests, and ultimately develop an understanding of the mechanism of the effect of an environmental factor. This thesis focuses on the development of a comprehensive numerical model used to describe the calcium-signaling pathway that can be applied to various cell types and processes.

The calcium (Ca^{2+}) ion is an important second messenger essential for eukaryotic life. [1] Calcium oscillations are important in carrying information from an extracellular agonist to facilitate a process. These intracellular Ca^{2+} oscillations are observed in a large variety of cell types and control various cellular processes. [1] The study of Ca^{2+} dynamics involves the

exchange of Ca^{2+} between intracellular stores and the cytosol, the interior and exterior of cells, and between cells. Further, the binding of Ca^{2+} to Ca^{2+}-binding proteins, pumps, and channels is also considered. Information is carried in the frequency (F) of Ca^{2+} oscillations and thus, theoretical models describing these oscillations provide information necessary to understanding the Ca^{2+}-signaling pathway.

B. Description of Calcium Oscillations:

Many processes in living cells are oscillatory. Obvious examples include the beating of the heart, lung respiration, and the activities of cell-cycle related enzymes such as cyclic adenosine monophosphate (cAMP). [2] The existence of Ca^{2+} oscillations in periodically contracting muscle cells and neurons has been known for a long time. [2] The earliest evidence of calcium oscillations came from experimentally supported studies on fluctuations of Ca^{2+}-dependent membrane properties. [3] The term “oscillations” can be used to describe all regular fluctuations in cytosolic Ca^{2+} concentration, which is the result of the nonlinearity of the dynamics of cytosolic Ca^{2+} concentration due to induced Ca^{2+} release in a single cell represented in **Figure 1**. [2]

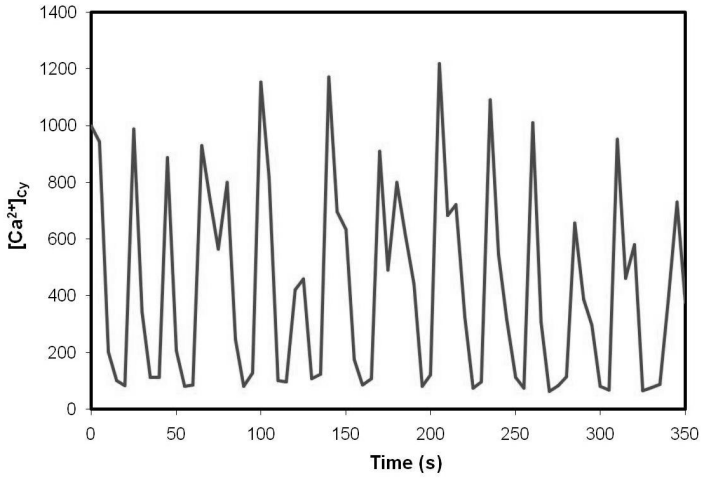

Figure 1. Calcium concentration (nM) over time obtained using the combined model (ComMeNT) with applied correlated noise (F = 0.0439 Hz)**.**

Multiple factors cause the overshoot in cytosolic Ca^{2+} concentration represented in **Figure 1**. The first is the influx of calcium through a voltage-gated calcium channel, the second is the passive influx of Ca^{2+} through imperfections in the membrane, and lastly, the release of calcium into the cytosol through IP_3-Receptor (IP_3-R). [2] Despite these factors, cytosolic Ca^{2+} concentration cannot remain elevated. As a result, the pumping of Ca^{2+} into the endoplasmic reticulum (ER), along with the efflux of Ca^{2+} from the cell causes cytosolic Ca^{2+} concentration to decrease. [2] This decrease marks the down shoot of the oscillatory trace in **Figure 1**. The repetition of these processes gives rise to the oscillatory behavior of cytosolic Ca^{2+} concentration. When cytosolic Ca^{2+} concentration is constant, or does not oscillate, this is considered the steady state condition.

Mathematical modeling is necessary in order to determine the requirements for this oscillatory behavior. The numerical integration of differential equations allows researchers to find the parameter range in which the state of cytosolic Ca^{2+} is not in steady state. [2] When the state of cytosolic Ca^{2+} concentration is not in steady state, Ca^{2+} oscillations are observed. These

two numerical regions, oscillatory and steady-state, are therefore vital to the study of intracellular Ca^{2+} dynamics and are demonstrated using mathematical models.

C. History of Minimal Models of the Ca^{2+}-signaling Pathway:

The comprehensive numerical model that was developed is based on two models that exist in the literature. The first model is a receptor operated model developed by Cuthbertson and Chay (CC model)[4], and the second model is a Ca^{2+}- induced Ca^{2+}-release (CICR) model developed by Borghans, Dupont, and Goldbeter (BDG model). [1] Both models are robust enough to represent fundamental characteristics of Ca^{2+} dynamics; however do not comprehensively discuss the overall process. The Ca^{2+}-signaling pathway can be divided into two parts. As a result, the numerical model for intracellular Ca^{2+} oscillations is divided in the same manner. The CC model reflects the first half of the process and the BDG model reflects the second half. The biological schematic of this Ca^{2+} signaling pathway is represented in **Figure 2**.

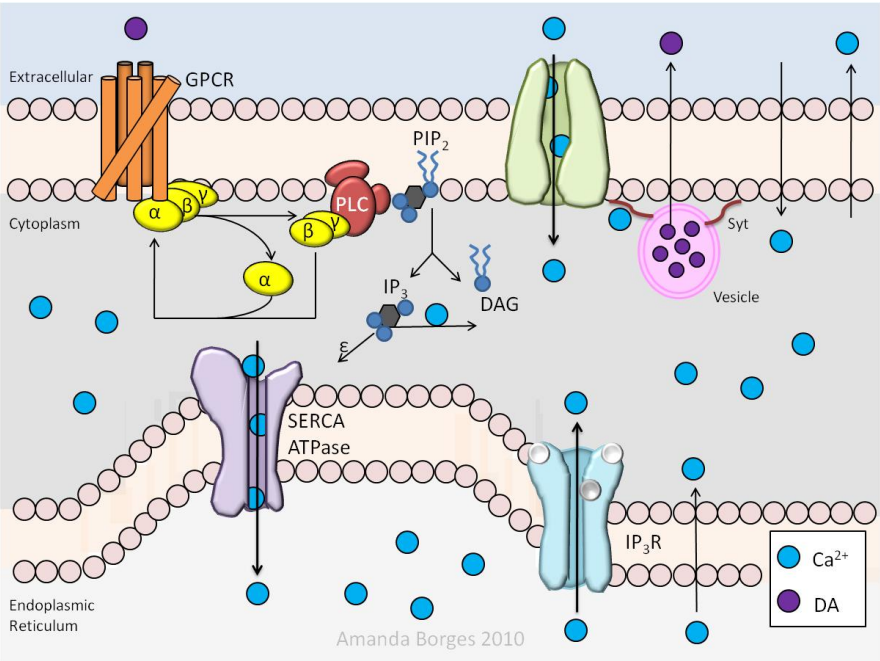

Figure 2. Biological representation of the Ca2+-signaling dependent secretion of dopamine release.

Once an agonist binds to a receptor on a cell, it triggers a G-protein cascading mechanism, which ultimately triggers Ca^{2+} influx through voltage-gated calcium channels. The primary focus of the CC model reflects this behavior. The model is considered "receptor-operated" because it was developed to account for the dependence of Ca^{2+} oscillations on the receptor type depending on the shape and the duration of free Ca^{2+} transients. [4] Specifically, Ca^{2+} oscillations are activated by GTP-binding proteins, which along with positive-feedback processes, leads to the activation of phospholipase C (PLC). [4] The activation of the effector protein PLC cleaves phosphotidylinositol-4,5-biphospate (PIP_2) to produce inositol-1,4,5-triphosphate (IP_3) and diacylglycerol (DAG). [4] This entire flow of events is represented by only one parameter (β) in the BDG model. [1]

Consequently, the BDG model represents the mechanism of Ca^{2+} oscillations after the events represented by β have occurred. The model is considered to be based on Ca^{2+}- induced Ca^{2+}-release because it represents the effect of cytosolic Ca^{2+} concentration on the IP_3-R of the ER which is responsible for the release of Ca^{2+} into the cytosol. [1] This phenomenon is called CICR because Ca^{2+} binding to the IP_3-R is responsible for the release of additional Ca^{2+} into the cytosol. All of the changes in cytosolic Ca^{2+} concentration represented by these two models account for the Ca^{2+} oscillations necessary for various processes to occur, therefore, combining the models provides scientists with a comprehensive and realistic account for the transmission of information through a cell by Ca^{2+}. Combining the models also accounts for the limitations in each of the models.

II- Analysis of Minimal Models

A. The CC Model:

The schematic for the receptor-operated CC Model is represented in **Figure 3 (a-b)**. The initiation of the reactions in this model is represented by the G-protein cascading mechanism in **Figure 3(b)**. The G-protein is split into three subunits, α, β, and γ. First, the α-subunit of the G-protein interconverts between the inactive GDP-bound form and the active GTP-bound form. [5] Phospolipase C is the effector protein which cycles between an inactive state (PLC) and an active state (*PLC). [5] Next, *PLC converts PIP_2 into two second messengers, IP_3, which participates in the process of releasing Ca^{2+} from intracellular stores, and DAG, which phosphorylates phosphokinase C (PKC). [5]

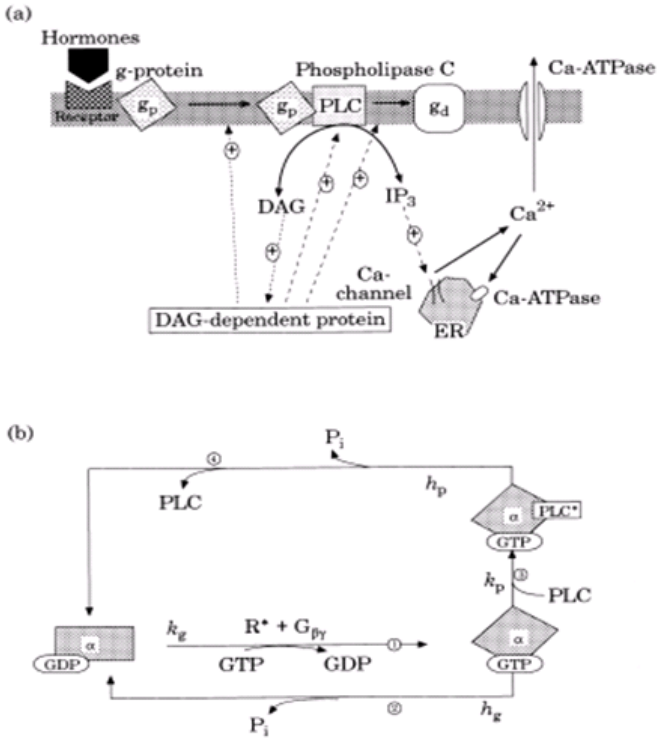

Figure 3. (a) Schematic representation of the one pool receptor-operated CC model. (b) Schematic representation of the receptor-initiated G-protein cascading mechanism responsible for the production of IP_3 and DAG. [5]

The core of the model is constructed by 4 differential equations that are dependent on the mechanisms discussed above. The equations are as follows: [5]

$$\frac{\mathrm{d}[\mathrm{G}\alpha\text{ - GTP}]}{dt} = k_g[G\alpha - GDP] - 4k_p[G\alpha - GTP]^4[PLC] - h_g[G\alpha - GTP] \quad (1)$$

$$\frac{d[DAG]}{dt} = k_d[PLC^*] - h_d[DAG] + l_d \quad (2)$$

$$\frac{d[Ca^{2+}]_i}{dt} = \rho\{k_c \frac{[IP_3]^3}{K_s^3 + [IP_3]^3} - h_c[Ca^{2+}]_i + l_c\} \quad (3)$$

$$\frac{d[PLC^*]}{dt} = k_p[G\alpha - GTP]^4[PLC] - h_p[PLC^*] \quad (4)$$

$$[G\alpha - GDP] = G_0 - [G\alpha - GTP] - 4[PLC^*] \quad (5)$$

$$[PLC] = P_0 - [PLC^*] \quad (6)$$

Equation (1) represents the change of the α-subunit bound active GTP concentration ([Gα-GTP]) over time. [5] The first term represents the production of Gα-GTP by the conversion from [Gα-GDP], the second term represents the loss of Gα-GTP in the activation of PLC to PLC*, and the third term represents the hydrolysis of Gα-GTP back to Gα-GDP. [5] Equation (2) characterizes the productions of DAG ([DAG]) and IP_3 ([IP_3]). Although explicitly stated as DAG, the concentration of IP_3 is assumed to be equal. The first term in this equation represents an increase in these two species due to the activation of PLC, the second term is the hydrolysis of the species, and the third term is a leak, which keeps the concentration of these species at a basal level. [5]

Equation (3) describes the change of cytosolic Ca^{2+} concentration ($[Ca^{2+}]_i$). In this equation, ρ represents a buffer system. [5] The first term inside of the curly brackets is the increase of $[Ca^{2+}]_i$ due to the release from the ER, the second term is the decrease of $[Ca^{2+}]_i$ due to its pumping back into the ER, and lastly, the third term is a leak which keeps $[Ca^{2+}]_i$ at a basal level. [5] The concentration of PLC* ([PLC*]) over time represented in equation (4) is described by the first term, which is the activation of PLC by Gα-GTP, and the second term, which is the loss of PLC* due to the inactivation of the complex and the formation of Gα-GDP. [5] Equations (5) and (6) represent the stoichiometry necessary to calculate Gα-GDP and PLC from the activated Gα-GTP and PLC* forms. Also important to note in this model, k_g, found in equation (1), is the parameter, which represents the agonist binding to the receptor on the membrane. [5]

B. The BDG Model:

Three variables are considered in this one pool CICR model, cytosolic calcium concentration ($[Ca]_{Cy}$), calcium concentration in the endoplasmic reticulum ($[Ca]_{ER}$), and the concentration of IP_3 ($[IP_3]$). [1] This model is depicted in **Figure 4**.

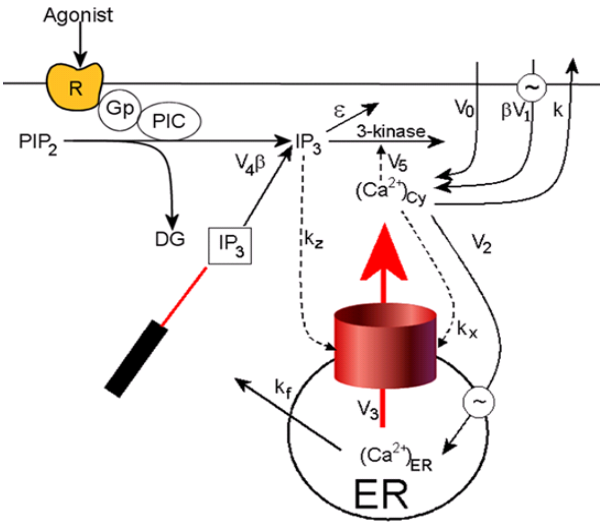

Figure 4. Schematic representation of the one pool BDG model based on CICR. [1]

Changes in $[Ca]_{Cy}$, $[Ca]_{ER}$, and $[IP_3]$, are denoted by parameters represented in the following differential equations: [1]

$$\frac{d[Ca]_{Cy}}{dt} = V_0 + V_1\beta - V_2 + V_3 + k_f[Ca^{2+}]_{ER} - k[Ca^{2+}]_{Cy} \quad (7)$$

$$\frac{d[Ca]_{ER}}{dt} = V_2 - V_3 - k_f[Ca^{2+}]_{ER} \quad (8)$$

$$\frac{d[IP_3]}{dt} = V_4\beta - V_5 - \varepsilon[IP_3] \quad (9)$$

With:

$$V_2 = V_{m2}\frac{[Ca^{2+}]_{Cy}^2}{k_2^2 + [Ca^{2+}]_{Cy}^2} \quad (10)$$

$$V_3 = V_m\frac{[Ca^{2+}]_{Cy}^m}{k_x^m + [Ca^{2+}]_{Cy}^2}\frac{[Ca^{2+}]_{ER}^2}{k_y^2 + [Ca^{2+}]_{ER}^2}\frac{[IP_3]^4}{k_z^4 + [IP_3]^4} \quad (11)$$

$$V_5 = V_{m5}\frac{[Ca^{2+}]_{Cy}^n}{k_d^n + [Ca^{2+}]_{Cy}^n}\frac{[IP_3]^p}{k_5^p + [IP_3]^p} \quad (12)$$

According to equation (7), $[Ca]_{Cy}$ changes over time due to the passive influx of Ca^{2+} (V_0), the DAG stimulated influx of Ca^{2+} through a voltage gated calcium channel ($V_1\beta$), the pumping of Ca^{2+} into the ER (V_2), the release of Ca^{2+} through the IP_3-R on the ER (V_3), the passive efflux of Ca^{2+} from the ER ($k_f[Ca^{2+}]_{ER}$), and the passive efflux of Ca^{2+} from the cytosol ($k[Ca^{2+}]_{Cy}$). [1] According to equation (8), $[Ca]_{ER}$ changes over time due to the pumping of Ca^{2+} into the ER (V_2), the release of Ca^{2+} through the IP_3-R on the ER (V_3), and the passive efflux of Ca^{2+} from the ER ($k_f[Ca^{2+}]_{ER}$). [1] Lastly, according to equation (9), the concentration of IP_3 over time is dependent on the production of IP_3 ($V_4\beta$), the Ca^{2+}-dependent degradation of IP_3 (V_5), and the calcium-independent degradation of IP_3 ($\varepsilon[IP_3]$). [1] Parameters V_2, V_3, and V_5 represented by

equations (10), (11), and (12) respectively, are hill functions denoted by exponents that reflect the cooperativity effect in which multiple ions of each species must bind in order for the process to occur. Further, the parameter β in equations (7,9) represents the DAG stimulated Ca^{2+} entry from the extracellular medium. [1]

C. Limitations within the Minimal Models:

The CC model includes an agonist-initiated production of DAG and a simplistic description of the Ca^{2+} dynamics between the ER and the cytosol. One of the first limitations is that the model assumes the concentrations of DAG and IP_3 are equal. This assumption is represented in equation (2). Although, the rate of production of DAG and IP_3 are equal (k_d[PLC*]), their paths of degradation are different and therefore their concentrations are not necessarily equal. Also, there is a simplistic description between the ER and the cytosol which is represented by equation (3). In this equation, the first term in the curly brackets, accounts for the regulation of the IP_3 receptor on the ER by IP_3, but it does not account for the necessary binding of Ca^{2+} to the receptor. In addition, the pumping of Ca^{2+} into the ER is described in a linear term. Further, a scaling factor (ρ) is placed into equation (3) to arbitrarily make the model work.

The BDG model, however, accounts for the dynamics between the ER and the cytosol in more detail. This detail is characterized by all three equations (7-9). In particular, $[Ca]_{ER}$ is calculated explicitly in equation (8). In addition, terms V_2 an V_3 in equations (10) and (11) reflect the exchange of Ca^{2+} between the cytosol and the ER. Term V_2, accounts for the binding of Ca^{2+} on the IP_3-R, and term V_3 accounts for the nonlinear dependence of Ca^{2+} pumping into the ER. One limitation of the BDG model is that the entire CC model, which was previously described, is incorporated within the single parameter β. The parameter β reflects the agonist

binding triggered cascading mechanism response portrayed in **Figure 3(b)**. In addition, similar to the CC model, the concentrations of DAG and IP_3 are assumed to be equal in the BDG model. In this case, the $[IP_3]$ is explicitly calculated and [DAG] is assumed equal.

III- Development of a Comprehensive Model

A. Comprehensive Model Iteration 1 (CoMBe):

A comprehensive model was developed in order to minimize the limitations of the minimal models previously described in this thesis. The model is called CoMBe and is represented in **Figure 5**.

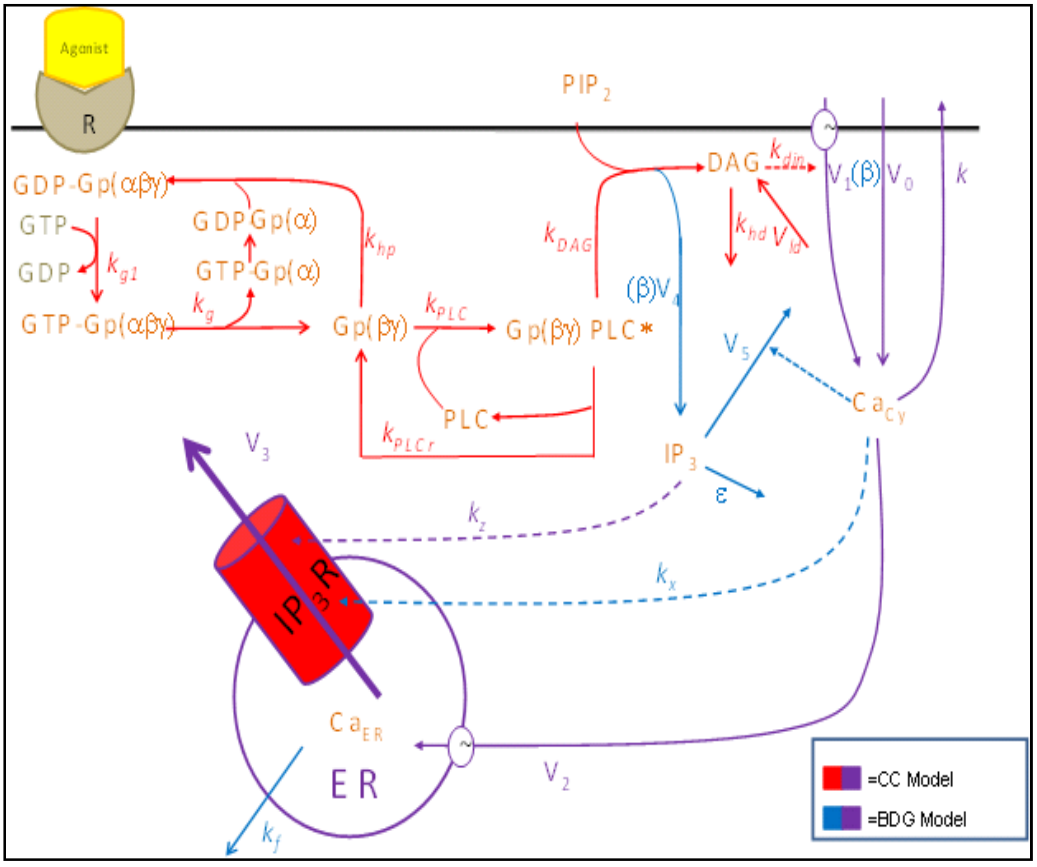

Figure 5. Schematic representation of CoMBe. Color-coding refers to models in which the parameters were taken.

The model is color coded according to the original models from which the parameters were taken. Parameters in red come from the CC model, and parameters in blue come from the BDG model. Purple parameters represent species that were accounted for in both models. In other words, to observe the CC model individually and in its entirety in CoMBe, both the red and purple parameters must be considered. Likewise, to observe the BDG model individually and in its entirety in CoMBe, both the blue and purple parameters must be considered.

The differential equations for this model are as follows:

$$\frac{d[Ca]_{Cy}}{dt} = V_0 + V_1 - V_2 + V_3 + k_f[Ca^{2+}]_{ER} - k[Ca^{2+}]_{Cy} \quad (13)$$

$$\frac{d[Ca]_{ER}}{dt} = V_2 - V_3 - k_f[Ca^{2+}]_{ER} \quad (14)$$

$$\frac{d[IP_3]}{dt} = V_4 - V_5 - \varepsilon[IP_3] \quad (15)$$

$$\frac{\mathrm{d[G}\alpha\text{ - GTP]}}{dt} = k_g[G\alpha - GDP] - 4k_{PLC}[G\alpha - GTP]^4[PLC] - k_{hg}[G\alpha - GTP] \quad (16)$$

$$\frac{d[DAG]}{dt} = k_{DAG}[PLC^*] - k_{hd}[DAG] + V_{ld} \quad (17)$$

$$\frac{d[PLC^*]}{dt} = k_{PLC}[G\alpha - GTP]^4[PLC] - k_{hp}[PLC^*] \quad (18)$$

$$V_1 = k_{DIN}[DAG] \quad (19)$$

$$V_2 = V_{m2}\frac{[Ca^{2+}]_{Cy}^2}{k_2^2 + [Ca^{2+}]_{Cy}^2} \quad (20)$$

$$V_3 = V_m \frac{[Ca^{2+}]_{Cy}^m}{k_x^m + [Ca^{2+}]_{Cy}^2} \frac{[Ca^{2+}]_{ER}^2}{k_y^2 + [Ca^{2+}]_{ER}^2} \frac{[IP_3]^4}{k_z^4 + [IP_3]^4} \quad (21)$$

$$V_4 = k_{DAG}[PLC^*] \quad (22)$$

$$V_5 = V_{m5} \frac{[Ca^{2+}]_{Cy}^n}{k_d^n + [Ca^{2+}]_{Cy}^n} \frac{[IP_3]^p}{k_5^p + [IP_3]^p} \quad (23)$$

$$[G\alpha - GDP] = G_0 - [G\alpha - GTP] - 4[PLC^*] \quad (24)$$

$$[PLC] = P_0 - [PLC^*] \quad (25)$$

Equations (13-15) are taken from the BDG model and equations (16-18) are taken from the CC model. Differential equation (13) is taken completely from the BDG model, therefore this adjustment minimizes the limitation of the rate of change of cytosolic Ca^{2+} concentration previously discussed in the CC model. Further, as previously mentioned, the CC model does not have a detailed description of the dynamics between Ca^{2+} and the ER. The first term in the curly brackets of equation (3) of the CC model is completely replaced by the parameter that accounts for the cooperativity effect on the IP_3-R (V_3).

Additionally, differential equations for [IP_3] and [DAG] are explicitly stated in this model and not assumed equal (equations (15, 17)). Separating these two species into two differential equations better represents the concentration of each species as a separate entity with its own formation and degradation path. In addition, the stimulation by the agonist is represented in this model by the parameter k_g, which replaces β. As a result, parameters V_1 (the influx of calcium through the voltage-gated Ca^{2+} channel), and V_4 (the production of IP_3 and DAG) were altered to

reflect this elimination (equations (19, 22)). Experimental support for this model is described later in this thesis.

B. Comprehensive Model Iteration 2 (ComMeNT):

The comprehensive mechanism CoMBe is a feasible model, which represents the individual processes of the Ca^{2+} signaling pathway. In order to further test the model, however, the mechanism was altered to describe a particular Ca^{2+}-dependent signaling mechanism. The new model depicted in **Figure 6**, a Comprehensive Mechanism for Neurotransmitter release (ComMeNT), describes the mechanism of dopamine (DA) secretion from PC12 cells. A new color-code was applied to this model.

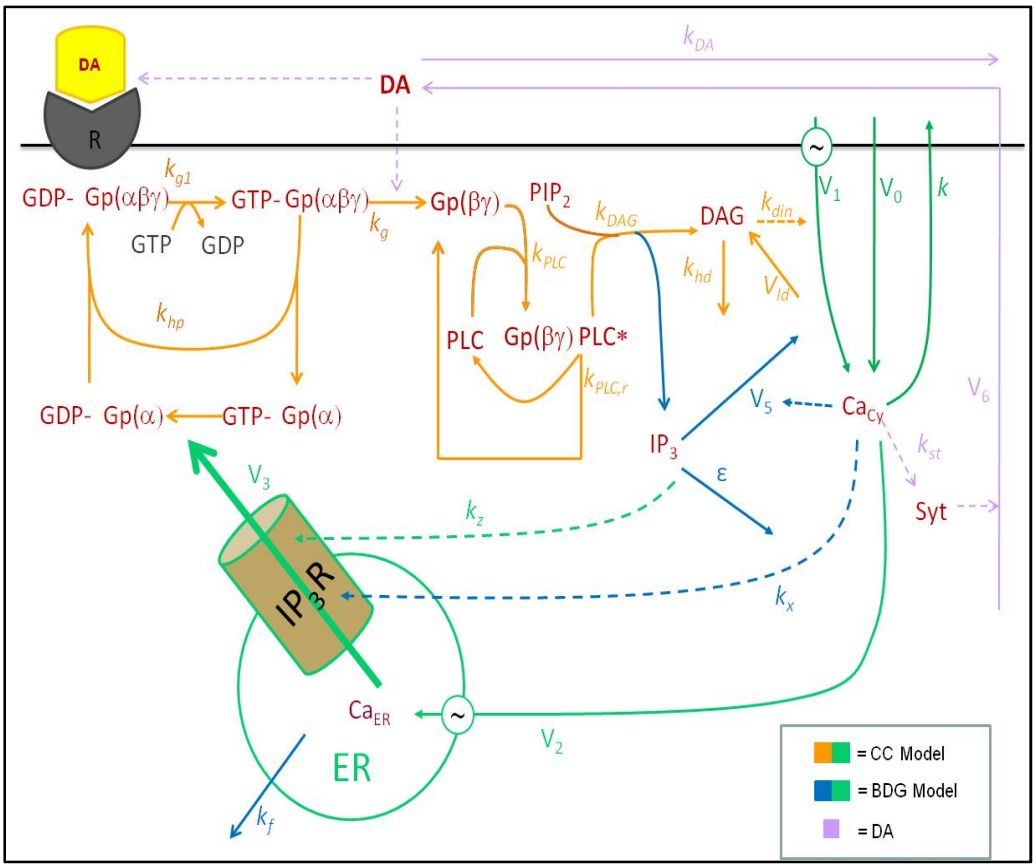

Figure 6. Schematic representation of ComMeNT. Color-coding refers to models in which the parameters were taken.

Parameters in orange come from the CC model, parameters in blue come from the BDG model, and green parameters represent species that were accounted for in both models. In other words, to observe the CC model individually and in its entirety in CoMBe, both the orange and green parameters must be considered. Likewise, to observe the BDG model individually and in its entirety in CoMBe, both the blue and green parameters must be considered. The equations and parameters from CoMBe are still used in this model, however, the new parameters which were added to the model to reflect DA secretion are light violet and are quantitatively expressed as follows:

$$\frac{d[DA]}{dt} = V_6 - k_{DA} - [DA] \tag{26}$$

$$V_6 = V_{m6} \frac{[Ca^{2+}]_{Cy}^2}{k_{st}^2 + [Ca^{2+}]_{Cy}^2} \tag{27}$$

$$k_g = k_{DAS} \frac{[DA]}{k_{D0} + [DA]} \tag{28}$$

Equation (26) reflects the rate of change of DA concentration over time ([DA]). The first term represents the release of DA from synaptic vesicles. This release is dependent on calcium concentration and the binding of synaptotagmin accounted for in the definition of V_6 (equation (27)). Lastly, k_g (the binding of the agonist to the receptor) is now defined as a hill function dependent on the concentration of DA as seen in equation (28).

IV- Experimental Verification for the Comprehensive Theoretical Models

A. Experimental Support for ComBe:

In order to test the feasibility of the first approach to the comprehensive mechanism for intracellular Ca^{2+} oscillations, existing experimental data was compared to theoretical data collected using the new model. The experimental data was provided from the master's thesis of Dr. Steven B. Symington and is represented in **Figure 7**. In his experiment, the effect of deltamethrin on voltage gated Ca^{2+} channels was studied. [6] Results indicate that treatment with deltamethrin increases cytosolic Ca^{2+} concentration in resting and depolarized states. [6]

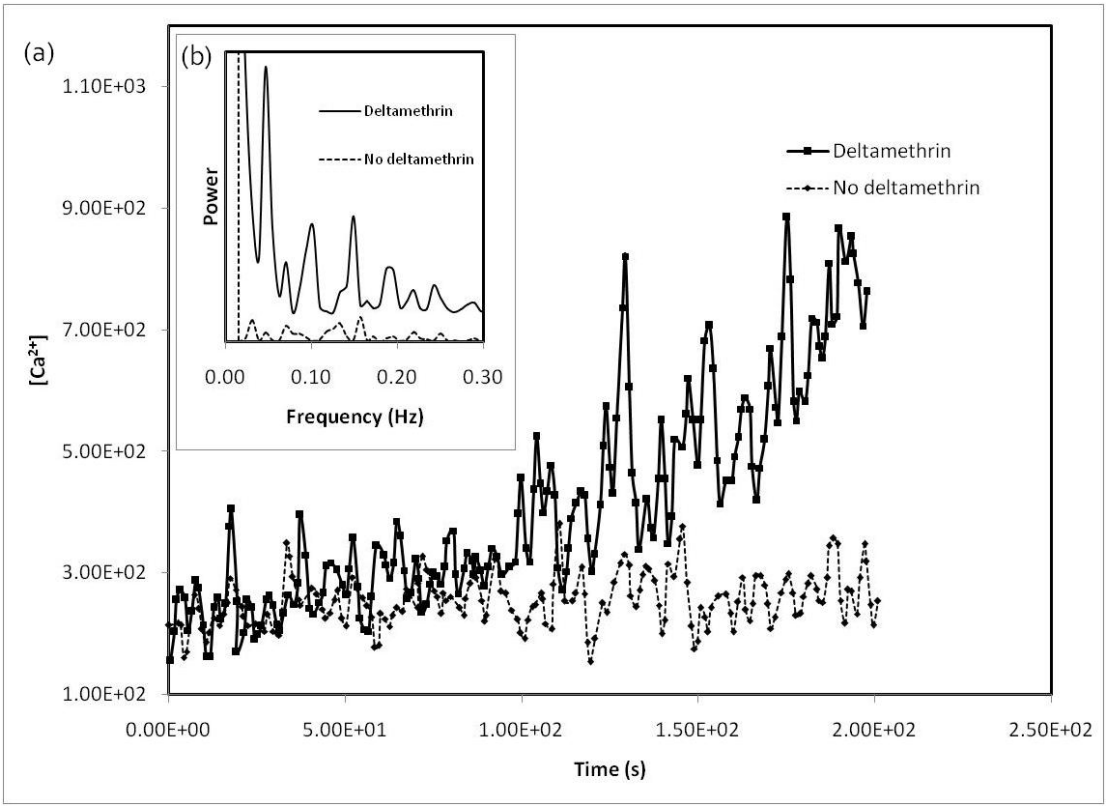

Figure 7. (a) The effect of ethanol and deltamethrin on calcium channels. Deltamethrin increases calcium concentration in resting and depolarized states. (b) Fast Fourier Transform (FFT) diagram. (F= 0.047 Hz). [6]

There were several qualitative patterns in these results that suggested a hypothesis could be developed and supported by ComBe. It was hypothesized that the model would successfully mimic specific patterns of behavior observed in Dr. Symington's experiments with *Paramecium* cells. It was hypothesized that if the model was feasible, cytosolic Ca^{2+} oscillations would occur at a sustained average before a reflected treatment with deltamethrin. Further, cytosolic Ca^{2+} concentration would increase until the concentration was too high and cell death occurred once the treatment with deltamethrin was applied. **Figure 8** represents the reconstructed qualitative patterns of the experimental data. In order to obtain this data a couple parameters were altered in the differential equation system. An adjustment at a particular time was made to k_g increasing its value to reflect treatment with deltamethrin. At a later time, an adjustment increasing the value of k_{din} was made to reflect K^+ depolarization.

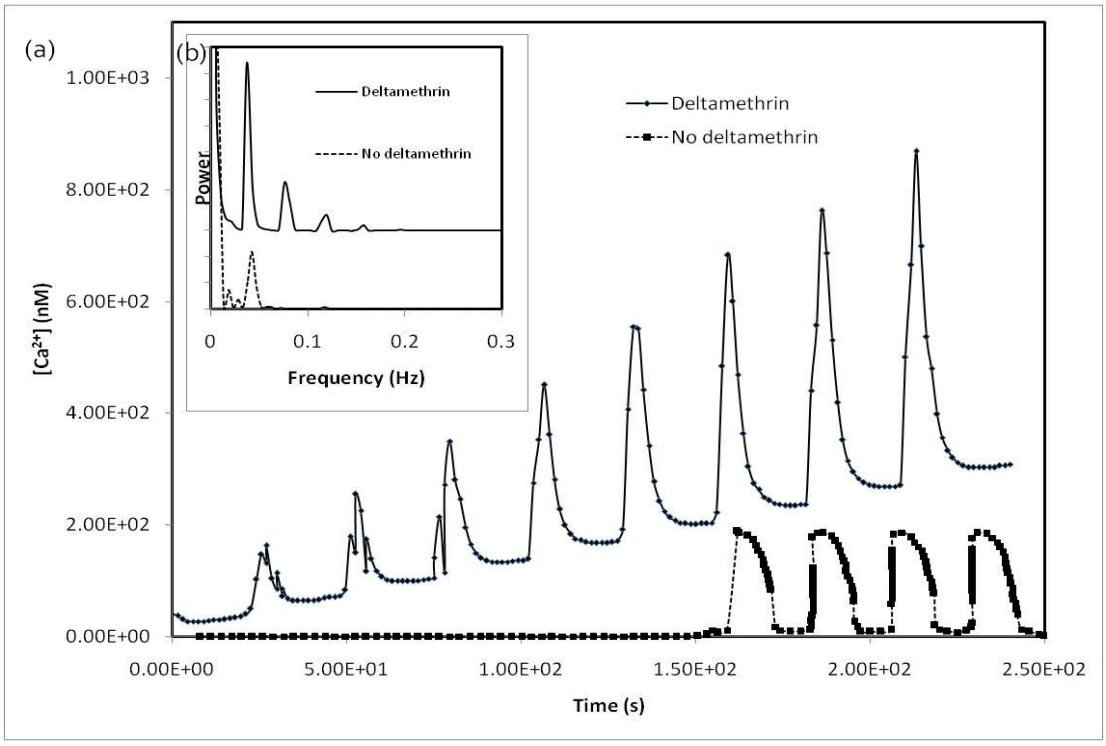

Figure 8. (a) Reproduction of the effect of deltamethrin on calcium channels. Adjustment of k_{din} reflects increasing calcium concentration in resting and depolarized states (b) FFT (F = 0.038 Hz).

In the theoretical results, deltamethrin treatment caused an increase in cytosolic Ca^{2+} concentration and therefore the theoretical results mimic the pattern of the experimental results. Qualitatively, these results suggest that our model is feasible and can be used to predict other cellular processes such as DA secretion. In addition, the frequency of the Ca^{2+} oscillations was matched both experimentally and theoretically using a Fast Fourier Transform (FFT) (**Figure 7(b), 8(b)**). The information carried by the Ca^{2+} oscillations is carried by the frequency, and therefore it was necessary to verify if the theoretical data represented the same signal as the experimental data. Due to random fluctuations within a cell *in vivo*, the frequency of Ca^{2+} oscillations varies between 0.01 and 0.1. Therefore, because the frequency obtained from the experimental data was 0.047 Hz, and the frequency of the theoretical data was 0.038 Hz, it was concluded that the experimental data supported the theoretical model and that the model was feasible.

B. Experimental Support for ComMeNT:

The second version of the model was used to understand the mechanism of Ca^{2+}-dependent DA release from PC12 cells. This signaling mechanism was chosen because of available experimental data on [DA] and PC12 cells in the biology department of Salve Regina University. This work involved measuring cytosolic Ca^{2+} concentration in PC12 cells by loading the cells with calcium green and measuring fluorescence. As a result, values of cytosolic Ca^{2+} concentration over time were provided for matching to data from the theoretical model (**Figure 9**).

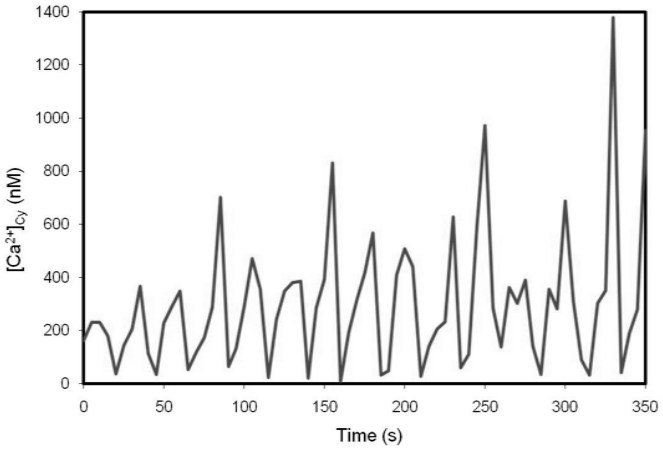

Figure 9. Calcium concentration (nM) over time obtained experimentally (F = 0.0437 Hz)**.**

Using this data, and the cytosolic Ca^{2+} concentration determined with the theoretical model (**Figure 1**) a FFT analysis was performed. The FFT for the experimental data is represented in **Figure 10** and the FFT for the theoretical data is represented in **Figure 11**.

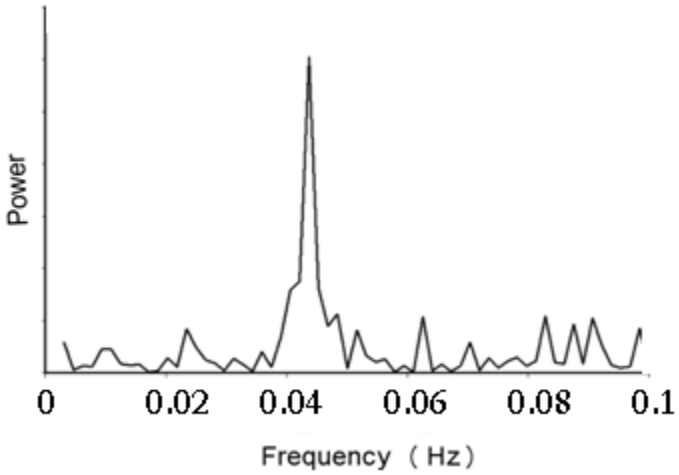

Figure 10. FFT of experimental data (F = 0.0437 Hz)**.**

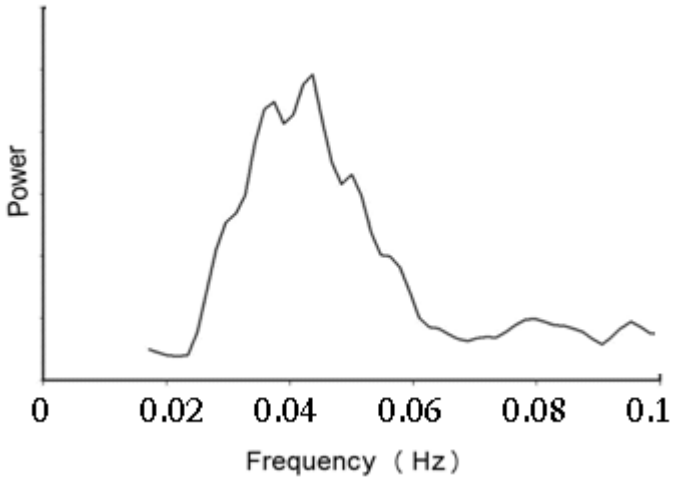

Figure 11. FFT of theoretical data (F = 0.0439 Hz)**.**

According to the FFT analysis, the model appears to be feasible because the same frequency is reflected in both the experimental and theoretical data within the normal variation.

In addition to monitoring cytosolic Ca^{2+} concentration, the effects of various DA treatments were observed. The results of these treatments are reflected in **Figure 12** and **Figure 13**.

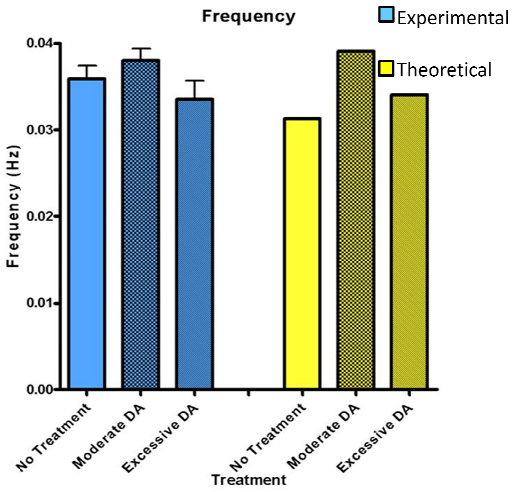

Figure 12. The effects of different treatments of DA on the frequency of cytosolic Ca^{2+} oscillations. Experimental data is blue, theoretical data is yellow.

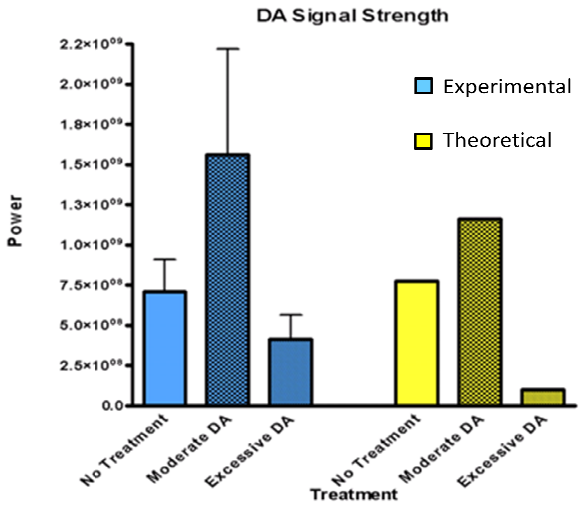

Figure 13. The effects of different treatments of DA on the transmission of the signal carried. Experimental data is blue, theoretical data is yellow.

The two treatments added to the cells were moderate DA treatment, and excessive DA treatment. A third group was used as a control with no DA treatment.

According to **Figure 12**, there was no relative difference in the frequency of cytosolic Ca^{2+} oscillations across the different levels of DA treatment. This was found for both the experimental and the theoretical data. This was an important conclusion because the information carried by the cytosolic Ca^{2+} oscillations is carried by the frequency. As a result, the information that is carried does not change because of the amount of DA in the cell. Experimental results support the dynamical behavior and the frequency of the oscillations predicted by the model.

Although the levels of treatment of DA did not affect the frequency of the oscillations, they did affect the quality of the signal that was carried. According to **Figure 13**, a moderate level of DA treatment optimized signal strength, and an excessive level of DA treatment degraded the quality of the signal. This information indicates that there is an optimal level of DA for the transmission of a signal, however once there is too much DA in the cell, the signal gets

corrupted. Theoretical results predicted the same dynamical behavior providing further support for the model.

V- Conclusion

A. The Mechanism of DA Secretion Can Be Studied Using the Comprehensive Model:

In summation, Ca^{2+} is an important second messenger for cellular communication. A comprehensive model was developed in order to minimize any limitations in the models currently presented in the literature. Experimental results support the model and therefore the theoretical model provides a plausible explanation of the dynamics of the Ca^{2+}-signaling mechanism. In the future, additional verification will be performed using various experimental configurations on PC12 cells. Further, the model will be used to predict the response of cells to environmental factors such as pesticides and heavy metals. The development of this model is relevant because multiple theoretical tests of pesticide testing can be done on the computer faster and cheaper than running actual experiments. In addition, the model will help scientists understand the effects that pesticides have on humans. This is vital because today, society depends on agriculture and the population is constantly exposed to multiple pesticides that have multiple active ingredients. Ultimately, the comprehensive model will help us understand the influence of these outside environmental factors, including toxins that are affecting the cellular communication mechanisms within our bodies.

Works Cited

1. Borghans, J.A.M., G. Dupont, and A. Goldbeter, *Complex intracellular calcium oscillations A theoretical exploration of possible mechanisms.* Biophysical Chemistry, 1997. **66**(1): p. 25-41.
2. Schuster, S. and M. Marhl, *Modelling of simple and complex calcium oscillations.* Eur. J. Biochem, 2002. **269**: p. 1333–1355.
3. Berridge, M.J., *Calcium oscillations*. 1990, ASBMB. p. 9583-9586.
4. Cuthbertson, K. and T. Chay, *Modelling receptor-controlled intracellular calcium oscillators.* Cell Calcium, 1991. **12**(2-3): p. 97.
5. Chay, T.R., Y.S. Lee, and Y.S. Fan, *Appearance of phase-locked wenckebach-like rhythms, devil's staircase and universality in intracellular calcium spikes in non-excitable cell models.* Journal of Theoretical Biology, 1995. **174**(1): p. 21-44.
6. Symington, Steven. *Characterization of the action of pyrethroids on the ciliary calcium channel of Paramecium tetraurelia.* Masters Thesis. 2000.